Durability Testing of Fluidized Bed Steam Reforming (FBSR) Waste Forms

C.M. Jantzen, T.H. Lorier, J.C. Marra, J.M. Pareizs
Savannah River National Laboratory
Aiken, SC 29808
USA

ABSTRACT

Fluidized Bed Steam Reforming (FBSR) is being considered as a potential technology for the immobilization of a wide variety of high sodium aqueous radioactive wastes. The addition of clay and a catalyst as co-reactants converts high sodium aqueous low activity wastes (LAW) such as those existing at the Hanford and Idaho DOE sites to a granular "mineralized" waste form that may be made into a monolith form if necessary. Simulant Hanford and Idaho high sodium wastes were processed in a pilot-scale FBSR at Science Applications International Corporation (SAIC) Science and Technology Applications Research (STAR) facility in Idaho Falls, ID. Granular mineral waste forms were made from (1) a basic Hanford Envelope A low-activity waste (LAW) simulant and (2) an acidic INL simulant commonly referred to as sodium-bearing waste (SBW). The FBSR waste forms were characterized and the durability tested via ASTM C1285 (Product Consistency Test, 10), the Environmental Protection Agency (EPA) Toxic Characteristic Leaching Procedure (TCLP), and the Single Pass Flow Through (SPFT) test. The durability of the FBSR waste form products was tested in order to compare the measured durability to previous FBSR waste form testing on Hanford Envelope C waste forms that were made by THOR^{sm} Treatment Technologies (TTT) and to compare the FBSR durability to vitreous LAW waste forms, specifically the Hanford low activity waste (LAW) glass known as the Low-activity Reference Material (LRM). The durability of the FBSR waste form is comparable to that of the LRM glass for the test responses studied.

INTRODUCTION

Fluidized Bed Steam Reforming (FBSR) is being considered as a potential technology for the immobilization of a wide variety of radioactive wastes but especially aqueous high sodium wastes at Hanford, Idaho National Laboratory (INL), and the Savannah River Site (SRS). The FBSR technology has been demonstrated to be effective at remediation of the following:

- Hanford LAW into a waste form, an Na-Al-Si (NAS) mineral product , for land disposal [1,2,3]
- Hanford LAW into carbonate or silicate form that can subsequently be vitrified [3]
- INL SBW into a carbonate form acceptable to the Waste Isolation Pilot Plant (WIPP) as a final waste form [1,4]
- SRS Tank 48 supernate with tetra phenyl borate (TPB) into either carbonates or silicates that are compatible with subsequent vitrification [5,6,7]; the Na and Si species can act as glass formers
- SRS salt supernates into carbonate, silicate, and/or NAS mineral forms for burial at SRS, WIPP, or Yucca Mountain dependent on the Waste Acceptance Criteria (WAC) of the disposal site.

The FBSR technology converts organic compounds to CO_2 and H_2O, converts nitrate/nitrite species to N_2, and produces the granular mineral waste form through reactions with superheated steam, which is the fluidizing media. The reforming process pyrolizes organics. Pyrolysis is not combustion as no oxygen gas is present. Therefore the FBSR technology has been determined to be Environmental Protection Agency (EPA) Clean Air Act (CAA) compliant by Region IV EPA, e.g. the Studsvik, Inc. commercial

Erwin facility. In addition, pilot scale testing by INL at the SAIC STAR facility has demonstrated that the FBSR process is Hazardous Waste Combustor (HWC) Maximum Achievable Control Technology (MACT) compliant for Hg, Cl, CO, total hydrocarbons [8] and other heavy metal constituents [9].

When clay is added to high sodium bearing waste the waste form produced is a multiphase mineral assemblage of Na-Al-Si (NAS) feldspathoid minerals with cage-like or ring like cavities, and iron bearing spinel minerals. The cage and ring structured minerals atomically bond radionuclides like Tc-99 and Cs-137 and anions such as SO_4, I, F, and Cl. Additional minerals that form such as ferrite spinels appear to stabilize Resource Conservation and Recovery Act (RCRA) hazardous species such as Cr and Ni [11,12].

The durability of the mineral waste forms produced during three different pilot scale FBSR demonstrations at the Science Applications International Corporation (SAIC) Science and Technology Applications Research (STAR) facility was evaluated in this study (Table I). The durability of the mineral waste forms was assessed against the mineral phases produced. The waste forms tested in this study (Table I) included the granular mineral material produced in the STAR fluidized bed after steady state operations were achieved and the finer mineral material from the filter, hereafter referred to as the filter fines. Bed material from the 2003 STAR pilot scale campaign with INL Sodium Bearing Waste (SBW) had not been optimized for NAS formation[1] while the 2004 pilot scale demonstration of SBW had been optimized for NAS formation. Both SBW pilot scale materials were tested with ASTM C1285 (Product Consistency Test).[10] In addition, bed and filter fines products from a third STAR pilot scale demonstration with a Hanford Low Activity Waste (LAW Envelope A) simulant were tested with ASTM C1285.[10] The LAW Envelope A and 2004 SBW bed products were also tested with the Single Pass Flow Through (SPFT) test. The SPFT and PCT durability of the LAW Envelope A bed product and fines from the STAR demonstration was compared to the durability of a bed product from a Hanford AN-107 (LAW Envelope C) demonstration performed by Studsvik, Inc., at Hazen Research in Golden, Colorado in 2001 (Table I). The results of the PCTand SPFT testing on the 2004 FBSR products and the comparisons between the 2001, 2003, and 2004 testing are discussed in this study.

The EPA Toxic Characteristic Leaching Procedure (TCLP) tests were also conducted on the LAW and SBW bed products. The TCLP test was performed on the 2004 FBSR bed products by an EPA certified laboratory (Acura Analytical Laboratory of Norcross, GA) and compared to the test results obtained by THOR^{sm} by an EPA certified laboratory (Evergreen in Golden Colorado) in 2001. Details of this comparison are given elsewhere [11,12].

NAS Mineral Waste Form Speciation

The formation of mineral waste forms by Fluidized Bed Steam Reforming (FBSR) has been demonstrated on an engineering scale for Hanford LAW supernates[,8,13] , and for INL Sodium Bearing Waste (SBW) [13]. Solid mineral phases were produced using a clay co-reactant. These sodium aluminosilicate (NAS) mineral waste forms are comprised of nepheline ($NaAlSiO_4$), and other feldspathoid mineral phases which have large cage-like structures formed of aluminosilicate tetrahedra that trap anion constituents such as Na_2SO_4 (nosean), NaI, NaCl (sodalite), NaF, Na_2MoO_4, $NaTcO_4$, $NaReO_4$. The cage structured feldspathoid system of minerals has the basic structural framework formula $Na_6[Al_6Si_6O_{24}]$. The square brackets in the formula are used to delineate the alumina:silica ratio of the aluminosilicate framework structure which is 1:1. The mineral nomenclature varies by the species that occupy the cage structure. The remaining feldspathoid minerals, such as nepheline, have a silica "stuffed derivative" ring type structure but the same $Na[AlSiO_4]$ framework structure.

[1] These tests were performed by INL before SRNL developed the compositional process control strategy spreadsheet called MINeral CALCulation (MINCALC)

Table I. Pilot Scale FBSR Samples Characterized and Tested Between 2001-2004

Date Facility	Waste Clay	Sample ID	Total Operating Time (TOT)	Bed Turnover (%)	Description
Oct 2001 HAZEN [8]	LAW (Env.C) Snobrite	SCT02-098-FM	4.8 hrs	Scoping Test	Bed product
		PR-01 Fines	23.3 hrs	Production Run	Filter fines
July 2003 STAR [9]	SBW Snobrite	Bed 260	82 hrs	Unknown [a]	Dynamic bed product
		Bed 272	82 hrs	Unknown [a]	Dynamic bed product
		Bed 277	82 hrs	Unknown [a]	Dynamic bed product
Aug 2004 STAR [13]	LAW (Env. A) OptiKasT	Bed 1103	55.5 hrs	97.4	Dynamic bed product
		Bed 1104[b] Bed 1123[b]	55.5 hrs	99.7	Final bed product
		Fines 1125	55.5 hrs	100	Final filter fines
Oct 2004 STAR [14]	SBW Sagger XX	Bed 1173	100 hrs	92	Final bed product

[a] unknown due to two defluidizing events that required a new starting bed
b these are both final bed samples that were subsampled at different times, Bed 1104 was used for PCT testing and Bed 1123 was used for SPFT testing

The feldspathoid mineral, sodalite has the formula $Na_8[Al_6Si_6O_{24}](Cl_2)$. The cage is occupied by two sodium and two chlorine ions [15]. The formula can also be written as $Na_6[Al_6Si_6O_{24}]\cdot(2NaCl)$ to indicate that two NaCl are ionically bonded in the cavities of the cage structure while the remaining Na:Si:Al have a 1:1:1 stoichiometry [ ]. When the 2NaCl are replaced by one Na_2SO_4 in the cage, the mineral phase is known as nosean, ($Na_6[Al_6Si_6O_{24}](Na_2SO_4)$) which is one of the feldspathoid cage structured minerals found in the FBSR waste form. Since the Cl^-, $SO_4^=$, and/or S_2 are chemically bonded inside the sodalite cage structure, these species do not readily leach out of the respective FBSR waste form mineral phases.

Other minerals in the sodalite family (hauyne and lazurite), are also cage structured minerals that can accommodate either SO_4 or S_2 depending on the oxidation state of the sulfur during the steam reforming process. Sodalite minerals are known to accommodate beryllium (Be) in place of Al and S_2 in the cage structure along with Fe, Mn, and Zn, e.g. helvite ($Mn_4[Be_3Si_3O_{12}]S$), danalite ($Fe_4[Be_3Si_3O_{12}]S$), and genthelvite ($Zn_4[Be_3Si_3O_{12}]S$) [15]. These cage-structured sodalites were found as minor phases in High Level Waste (HLW) supercalcine[2] waste forms [16] and were found to retain Cs, Sr, and Mo in the cage-like structure, e.g., Mo as $Na_6[Al_6Si_6O_{24}](NaMoO_4)_2$ [16]. In addition, sodalite structures are known to retain boron [17], germanium [18], iodine [15,18] and bromine [15,18] in the cage like structures. Indeed, waste stabilization at Argonne National Laboratory-West (ANL-W) currently uses a glass-bonded sodalite ceramic waste form (CWF) for disposal of electrorefiner wastes for sodium-bonded metallic spent nuclear fuel from the EBR II fast breeder reactor that are enriched in NaCl [19,20].

[2] Supercalcines were the high temperature silicate based "natural mineral" assemblages proposed for HLW waste stabilization in the United States (1973-1985).

A second feldspathoid mineral found in the FBSR waste form is nepheline, $Na[AlSiO_4]$ [21]. Nepheline is a hexagonal structured feldspathoid mineral. The ring structured aluminosilicate framework of nepheline forms cavities within the framework. There are eight large (nine-fold oxygen) coordination sites and six smaller (8-fold oxygen) coordination sites in nepheline [ ]. The larger nine-fold sites can hold large cations such as Cs, K, and Ca while the smaller sites accommodate the Na. The K analogue is known as kalsilite ($K[AlSiO_4]$). The nepheline structure is known to accommodate Fe, Ti and Mg as well.

A sodium rich cubic structured nepheline $(Na_2O)_{0.33}Na[AlSiO_4]$ (PDF#39-0101) is also found in the FBSR NAS product. This nepheline structure has large (twelve-fold oxygen) cage like voids in the structure [22] for anion/radionuclide retention. Carnegieite ($Na[AlSiO_4]$) is a metastable form of nepheline that readily transforms upon heating at longer reaction times. While nepheline and carnegieite normally have an Al:Si ratio of 1:1, they can form a variety of structures that are either Si or Al deficient.

When an iron oxide co-reactant is added during FBSR processing, an AB_2O_4 spinel mineral known as magnetite forms. In magnetite the A lattice site is Fe^{2+} while the B lattice site is Fe^{3+}. However, substitutions of Mg^{2+}, Zn^{2+} Ni^{2+}, and Mn^{2+} in the A site are common and substitutions of Cr^{3+}, small amounts of Al^{3+}, and occasionally substitution of Ti^{4+} in the B site are common [15]. The +2 cations can randomly substitute for each other on the A lattice site and any of the +3 or +4 cations can substitute on the B lattice. The conversion of Cr^{6+} to Cr^{3+} at elevated temperatures and deoxygenated conditions and the stabilization of Cr^{3+} in $(Mg,Fe)(Fe,Al,Cr)_2O_4$ spinel has recently been investigated for the stabilization of Cr-rich industrial wastes in glass ceramics [23]. The stabilization of large concentrations of Cr^{3+} in the spinel phases produced in industrial waste glass ceramics have been shown to exhibit TCLP test responses that were orders of magnitude below the EPA regulatory Universal Treatment Standard (UTS) [24] limits necessitated for treated waste forms whether classified as characteristically hazardous or listed wastes under the Resource Conservation and Recovery Act (RCRA) Land Disposal Restrictions (LDR).

EXPERIMENTAL APPROACH

The approach used in this study was to chemically analyze the 2003 and 2004 STAR pilot scale bed and filter fines mineral products and characterize the minerals formed by X-ray Diffraction (XRD). The durability of the STAR pilot scale mineral products was tested with the Product Consistency Test (PCT or ASTM C1285-02, 10) and the Single Pass Flow Through (SPFT) test. The PCT and SPFT results are then compared to the mineral phases produced and to previous testing by THOR^{sm} on Hanford LAW waste.

Chemical Composition

Elemental and anion compositions of the steam reforming materials were measured. The charcoal was removed prior to analysis by heating the samples to 525°C overnight in air. This is the temperature specified in a United States Geological Survey (USGS) procedure [25] for carbon removal in preparation for analysis. Samples were examined by XRD to verify that the phase assemblages had not changed after heating. Solid samples were digested [see 26 and 27] and the resulting solutions were analyzed by Inductively Coupled Plasma Emission Spectroscopy (ICP-ES) and by ICP Mass Spectroscopy (ICP-MS). Anion content was determined from a sodium peroxide/sodium hydroxide fusion at 600°C followed by a water uptake [28]. The resulting solutions were analyzed by Ion Chromatography (IC) for NO_3^-, F^-, and Cl^-. The REDuction/OXidation (REDOX expressed as the iron (II) to total iron ratio) of the mineral product was determined [29] on samples where the charcoal was removed by hand so that heating in air to remove the charcoal would not oxidize the sample and changed the ratio.

Waste Form Surface Area (SA) and Durability Measurements

The Product Consistency Test (PCT) results can be expressed as a normalized concentrations (NC_i) which have units of $g_{waste\ form}/L_{leachant}$, or as a normalized release (NL_i) in $g_{waste\ form}/m^2$, or as a normalized rate (NR_i) in $g_{waste\ form}/ m^2 \cdot$day where "i" is the chemical element of interest. Expression of the PCT test response as NL_i, the standard units in which the LAW glass specification is given, necessitates the use of the surface area (SA) of the sample releasing species "i" and the volume (V) of the leachant being used which is expressed as the SA/V ratio:

$$NL_i = \frac{c_i(sample) - c_i^0(blank)}{f_i \bullet (SA/V)} \qquad \text{(Eq. 1)}$$

where NL_i is the normalized release ($g_{waste\ form}/m^2$)
c_i *(sample)* is the concentration of element *i* in the sample leachate solution (g_i/L)
c_i^0 *(blank)* is the concentration of element *i* in the blank leachate solution (g_i/L)
f_i is the fraction of element *i* in the unleached waste form ($g_i/g_{waste\ form}$)
SA/V is the surface area of the final waste form divided by the leachate volume (m^2/L)

SPFT experiments are designed to reach steady-state conditions between an aqueous solution (leachant) and the test material (waste form) by maintaining a constant solution pH and flow rate at constant temperature. Thus, in the SPFT test the elements are released into solution from waste form dissolution by continuously introducing fresh leachant into the system which maintains the chemical affinity term in the kinetic rate equations used to express dissolution near zero. By monitoring the change in the dissolution rate over a range of temperatures and pH values the kinetic terms, terms necessary for Performance Assessment (PA) modeling of waste forms such as the activation energy of dissolution can be determined. Therefore, for SPFT testing, the units of NR_i are used to accommodate the flow rate parameter, F. Normally the NR_i response is plotted against the number of days that the test has been performed [30]:

$$NR_i = \frac{c_i(sample) - c_i^0(blank)}{f_i \bullet (SA/F)} \qquad \text{(Eq. 2)}$$

where NR_i is the normalized release ($g_{waste\ form}/m^2 \bullet$day)
SA/F is the surface area of the final waste form in m^2 divided by the flow rate, F, in L/day

In order to calculate NL_i or NR_i, the surface area of the material being tested must either be calculated from particle size and density (ASTM C 1285, 10, Appendix XI) or measured. In this study, the waste form SA was measured by the Brunauer, Emmett, and Teller [31] (BET) using the N_2 gas method recommended by McGrail [1] due to the high surface roughness and high internal porosity of the FBSR product compared to vitrified waste form products (see 1,11,12,30). The charcoal was removed from the samples, the samples were sized and cleaned for durability testing before BET surface area measurement.

PCT and SPFT tests were performed on a charcoal free basis to remove non-leachable charcoal from the FBSR products. The unreacted charcoal dilutes the amount of each mineral species present in a gram of mineral product and contributes to the overall surface area [11,12]. Moreover, (1) the charcoal density is different than the mineral product density which would complicate the calculation of a geometric surface area since the proportion of charcoal vs. mineral product must be known, (2) the presence of charcoal skews the measured BET surface area to an irreproducible and high value which would make the FBSR product appear to be more durable [11,12], and (3) the charcoal will be removed in the tandem FBSR flowsheet developed by THOR^{sm} which was not a condition that was simulated in the single FBSR STAR

or Hazen pilot scale flowsheets. Hence, the charcoal was removed from the FBSR products before PCT and SPFT testing and the BET surface area measured on the charcoal free products.

In order to compare one sample to another both the PCT and the SPFT procedures call for control of several parameters that can otherwise cause irreproducible leachate responses. One of these parameters is the removal of electrostatically adhering particles which are removed by a 100% ethanol washing procedure. This step controls the Gaussian distribution of the particles needed to measure an "average" solution response for a given sample at a given mesh size and to be able to compare the test response to a different sample at that same mesh size. This is important when reporting in units of NLi when the test response is not normalized by the surface area as in Equations 1 and 2. While the nominal PCT test (PCT-A) conditions specify a -100 to +200 mesh size smaller mesh sizes than the nominal -100 to +200 mesh size are allowed as was done to test the FBSR fines in this study. For all samples, ASTM Type I water [32] was used as the leachant, a constant leachant to sample ratio of 10 cm^3/g or 0.01 L/g was used, the test temperature was 90°C, and the test duration was seven days. The test temperature, duration, and SA/V ratio are the test conditions used for testing glass waste form performance.

SPFT tests were used to quantify the dissolution kinetics of the FBSR bed products taken after steady state conditions were achieved in the FBSR during the 2004 STAR facility pilot scale demonstrations. One LAW and one SBW sample were tested. SPFT testing was performed at various 25°C, 40°C, 70°C, and 90°C, at a constant flow rate of 288 mL/day, with leachants at pH 7, 8, 9, 10, and 11 [1,30] for 3 to 14-days. For comparison McGrail et al. [1] tested various flow rates up to a maximum flow rate of 200 mL/day at the same 5 pH values but at only one temperature, 90°C for up to 23 days. The 288 mL/day flow rate was chosen for this study because of the expected decline in release rate with decreasing flow rate and to ensure there would be no feedback from the leachant solutions. Sampling began on the third day of each test in order to allow the system to reach steady-state conditions, and then continued every other day until the test completion on the 14^{th} day. Once collected, each sample was filtered through a 0.45 micron filter, analyzed for the concentrations of Si, Al, Na, and S via ICP-ES, and for Re via ICP-MS. The fate of S dissolved from the waste form is important because S limits waste loading in glass waste forms but not in the FBSR mineral product. The fate of Re dissolved from the waste form is important as it is a surrogate for Tc-99.

RESULTS

Characterization

The measured compositions of the STAR FBSR bed products and fines are given on a (carbon free) oxide basis in Table II. Oxide sums within 100±5 wt% indicate an excellent mass balance on a mineral oxide basis similar to the oxide basis on which glass formulations are reported. Elemental Fe in the oxide mineral FBSR product is speciated into FeO and Fe_2O_3 using the measured REDOX of the sample. An electromotive force (EMF) series developed for the FBSR product by Schreiber [33] allows the amount of Cr present as Cr^{n+} (n is chromium in a mixed oxidation state of +3, +4, +5) vs. Cr^{6+} to be determined. The measured REDOX ratios given in Table II when coupled with the EMF series indicates that 86% of the Cr in the STAR SBW 2003 FBSR product was Cr^{n+} , 78% of the Cr in the STAR LAW 2004 FBSR product was Cr^{n+}, and ~91% of the Cr in the STAR 2004 SBW FBSR product was Cr^{n+}. For comparison about 62% of the Cr in the Hazen 2002 FBSR product was Cr^{n+} based on the measured [2] REDOX ratio.
The X-ray diffraction analyses are given in Table III which allows identification of the various feldspathoid and spinel minerals. Table III indicates that there is excess Al_2O_3 in samples Bed 260 and Bed 1173 from the Al_2O_3 starting bed material. This prediction is consistent with the bed turnovers given in Table I. Table III indicates that there was incomplete reaction in the STAR 2004 SBW campaign

because beta alumina, $NaAl_{11}O_{17}$ along with unreacted SiO_2 and SiO_2 in the form of a different sodium calcium silicate (combeite) was identified.

Table II. Oxide and Anion (Sodium Salt) Mass Balance of Steam Reformer Bed Products and Fines †

Oxides (Wt%)	2003 SBW FBSR Products			2004 LAW FBSR Products			2004 SBW FBSR Products	2002 LAW FBSR Products		
	Bed 260	Bed 272	Bed 277	Bed 1103	Bed 1104	Fines 1125	Bed 1173	Bed AN-107 5/31/02 [2]	Bed AN-107 8/15/02 [2]	Fines PR-01
Al_2O_3	42.3	36.8	38.0	32.88	32.40	34.67	38.36	31.75	38.92	32.22
CaO	0.700	0.770	0.770	1.78	2.31	1.78	3.79	0.73	0.57	4.44
Cr_2O_3	0.00	0.00	0.00	0.13	0.12	0.10	0.10	0.07	0.03	0.04
Cs_2O	5.47×10^{-2}	9.44×10^{-2}	6.46×10^{-2}	1.51×10^{-4}	1.20×10^{-4}	1.82×10^{-3}	3.25×10^{-2}	2.9×10^{-3}	5.0×10^{-3}	1.38×10^{-3}
Cu_2O	NM	NM	NM	0.02	0.01	0.01	0.01	NM	NM	0.02
Fe_20_3	0.972	0.728	0.721	0.257	0.196	0.243	0.192	5.45	6.23	1.53
FeO	1.31	0.69	0.651	NM	0.068	NM	0.737	0.88	1.00	NM0
K_2O	2.65	3.60	3.67	0.33	0.30	0.31	3.96	0.70	0.68	1.49
La_2O_3	6.68×10^{-3}	6.68×10^{-3}	6.68×10^{-3}	6.68×10^{-3}	6.68×10^{-3}	6.68×10^{-3}	6.68×10^{-3}	1.17×10^{-3}	NM	6.68×10^{-3}
MgO	0.182	0.216	0.216	0.05	0.07	0.07	0.40	NM	NM	0.43
MnO	NM	NM	NM	0.04	0.04	0.04	0.36	NM	NM	0.22
Na_2O	14.7	17.1	16.8	19.85	19.57	21.42	16.42	19.82	16.78	22.67
NiO	NM	NM	NM	0.013	0.013	0.013	0.051	0.081	0.035	0.064
P_2O_5	1.83	2.39	2.13	0.481	0.458	0.458	0.859	0.218	0.247	0.504
Pb	NM	NM	NM	<0.1	<0.1	<0.1	<0.1	0.0248	0.0199	0.06
ReO_2	1.58×10^{-2}	2.42×10^{-2}	2.82×10^{-2}	6.60×10^{-3}	4.80×10^{-3}	4.63×10^{-3}	5.57×10^{-3}	5.0×10^{-4}	6.0×10^{-4}	1.82×10^{-3}
SiO_2	32.1	37.3	37.5	35.73	35.62	43.00	37.65	34.87	30.06	35.41
TiO_2	1.30	1.07	1.05	1.23	1.18	1.27	1.19	NM	NM	1.18
NaCl	<0.2	<0.2	<0.2	0.297	0.214	0.165	0.152	NM	0.524	0.152
NaF	<0.2	<0.2	<0.2	<0.2	<0.2	<0.2	<0.2	NM	NM	<0.2
NaI	NM	NM	NM	$<2 \times 10^{-5}$	$<2 \times 10^{-5}$	$<2 \times 10^{-5}$	NM	NM	NM	$<2 \times 10^{-5}$
Na_2SO_4	0.591	0.961	0.680	1.29	1.11	1.69	0.182	0.55	3.89	1.15
Sum	98.67	101.58	102.17	94.38	93.69	105.25	104.46	95.15	98.99	101.53
$Fe^{2+}/\Sigma Fe$	0.61	0.52	0.51	NM	0.28	NM	0.81	0.15	0.15	NM

† Results in this table are on a nitrate-free basis. Nitrate was detected in some of the bed product samples. If the nitrate for these samples (Bed 260, Bed 272, and Bed 277) were included in this table, the $NaNO_3$ content would be approximately 0.4 et%, and the Na_2O content would decrease by approximately 0.1%.

Table III. Mineral Phases Identified in the Pilot Scale Products Tested

	$NaAlSiO_4$ Carnegieite (PDF #11-0220)	$(K_{0.25}Na_{0.75})AlSiO_4$ K-substituted Nepheline (PDF#74-0387)	$Na_{0.89}Al_{0.9}Si_{1.1}O_4$ Si rich Nepheline (PDF#79-0993)	$NaAlSiO_4$ Nepheline (PDF#35-0424)	$Na_{1.53}Al_{0.92}Si_{0.92}O_4$ Na-rich Nepheline (PDF # 39-0101)	$Na_{1.45}Al_{1.45}Si_{0.55}O_4$ Si deficient Carnegieite (PDF#49-0002)	$Na_6[Al_6Si_6O_{24}](Na_2SO_4)$ Nosean (PDF#73-1734, 17-0535)	$Na_6[Al_6Si_6O_{24}](2NaCl)$ Sodalite (PDF #82-0517) Un-named Sodalite (PDF#42-0215)	Al_2O_3 (from Starting Bed) Corundum (PDF #74-1081, 42-1468, 10-0173)	TiO_2 (clay impurity) Anatase (PDF #21-1272)	SiO_2 (clay impurity) Quartz (PDF#85-1053)	$NaAl_{11}O_{17}$ Beta-Alumina (PDF# 76-0923)	$Na_{5.27}Ca_3(SiO_6O_{18})$ Combeite (PDF# 78-1650)	Fe_3O_4 (PDF#79-0416, #19-0629) Fe_2O_3 (PDF#33-0664)
July 2003 SBW CAMPAIGNS														
Bed 260		X				Y		TR	Y	TR				
Bed 272		X				Y		TR		TR				
Bed 277		X				Y		TR		TR				
August 2004 LAW CAMPAIGNS														
Bed 1103	X		X				Y			TR				
Bed 1104	X		X				Y			TR				
Fines 1125	X		TR							TR				
October 2004 SBW CAMPAIGNS														
Bed 1173		X						TR	Y		TR	TR	Y	
AN-107 2002 LAW CAMPAIGNS														
SCT02-098-FM				X	Y		Y		TR					Y
Fines PR-01	X			X			Y		Y					Y

X = Major constituent; Y = Minor constituent, TR = trace constituent

Surface Area to Volume Ratio

Table IV gives the measured BET surface areas measured in this study on a carbon-free basis (charcoal removed by roasting) and the value measured by McGrail et al.[1] (charcoal removed manually) for comparison. Although McGrail et al.[1] determined that the measured BET surface area should be used during the calculation of release rates for the FBSR product and the calculated geometric surface area should be used during the calculation of release rates for glass, the BET surface area was used for both waste forms in this study (Table IV) consistent with the recommendation of Knauss, et.al [34].

Product Consistency Test and Aluminosilicate Buffering

Three sets of samples from the INL FBSR campaigns were evaluated by the Product Consistency Test. The samples were (1) simulated SBW campaign products from July 2003, (2) LAW campaign products from August 2004, and (3) SBW campaign products from October 2004. Leachate concentrations were calculated from Equation 1 as normalized releases using the measured SA_{BET} (m^2/g) and plotted in Fig. 1. Data is given in reference 11.

The PCT final leachate pH values and the surface areas from Table IV are plotted in Fig. 1 and indicate that the final PCT solution pH is an inverse function of the sample SA_{BET} (m^2/g), e.g. the pH is lower for samples with a larger SA_{BET} (m^2/g). In addition, the pH appears to be related to the mineral phases present in the samples (see discussion about aluminosilicate buffering below). For example, the STAR 2004 LAW fines have a measured SA_{BET} (m^2/g) that is about the same as the SA_{BET} (m^2/g) measured for the 2004 LAW bed material, e.g. the sample microporosity is similar, but the solution pH values of the bed and the fines are very different. This indicates that the mineralogy, especially the Al:Si ratio of the mineral species formed may play a role in the FBSR mineral dissolution mechanism.

The inverse correlation of pH and SA is unusual: in low Al containing alkali borosilicate glasses the leachate pH increases as more alkali and hydroxide are released to solution from the higher surface of exposed glass. This release of alkali and hydroxide occurs during the early stages of glass dissolution by ion exchange. For the stoichiometric and non-stoichiometric nephelines/carnegieites (Table III) found in the STAR SBW 2003 and 2004 FBSR products and in the Hazen AN-107 campaigns the appropriate NAS ion exchange reaction at the start of a PCT test when the ASTM Type I water [32] pH is ~5.5 would be:

$$Na_xAl_ySi_zO_4 + (0.5x + 1.5y + z)H_2O \xrightarrow{90^\circ C} xNa^+ + zH_2SiO_3 + yAl(OH)_3 + x(OH)^- \qquad \text{(Eq. 3)}$$

The ion-exchange reaction shown in Equation 3 liberates hydroxide which drives the PCT leachates basic as a function of reaction time. Stoichiometric nepheline (where x=y=z=1) liberates one mole of OH^- for every mole of nepheline. The defect nephelines and carnegeites liberates between 0.9 to 1.53 moles of OH^-. Note that the Si-deficient and sodium rich nephelines liberate the most hydroxide per mole, e.g. 1.45-1.53 moles of OH^-, respectively. A similar mechanism may or may not be active for the incomplete reaction products beta alumina ($NaAl_{11}O_{17}$ and SiO_2; Table III) formed in the STAR 2004 SBW from incomplete reaction:

$$Na_xAl_yO_{17} + zSiO_2 + (0.5x + 1.5y + z)H_2O \xrightarrow{90^\circ C} xNa^+ + zH_2SiO_3 + yAl(OH)_3 + x(OH)^- \qquad \text{(Eq. 4)}$$

As the PCT test continues the solution changes from a pH of 5.5 to >10 and passes through different aqueous stability fields, e.g. $HSiO_3^-$, $SiO_3^=$ and $Al(OH)_4^-$. As the pH increases during PCT testing,

Equation 5 becomes dominant for the NAS phases (including the beta alumina plus SiO_2). Per Equation 5 different nepheline/carnegieite Na:Al:Si ratios complex different amounts of hydroxide as $Al(OH)_4^-$:

$$Na_xAl_ySi_zO_4 + (0.5x + 1.5y)H_2O + (y + z - x)OH^- \xrightarrow{90^\circ C} xNa^+ + zHSiO_3^- + yAl(OH)_4^- \qquad \text{(Eq. 5)}$$

Therefore, the leachate pH is particularly dependent on the amount of alumina present in the sample being tested and the amount of $Al(OH)_4^-$ formed in the leachate, i.e., the amount of OH^- complexed as $Al(OH)_4^-$. This can be confirmed graphically (Fig. 1b-c) by showing the strong dependence of the PCT normalized releases for the alkalis (Na and Cs) versus the normalized releases for alumina.

Since reactions 3 and 4 continue to produce hydroxide while reaction 5 continues to complex hydroxide as the aqueous $Al(OH)_4^-$ species, the pH continues to change depending on the relative rates of these two competing processes and the values of the atomic ratios of Na:Al:Si, e.g. *x*, *y*, and *z*. When the pH reaches 11.7, the stable silica species is $SiO_3^=$. At this point reaction 5 becomes dominant at 90°C:

$$Na_xAl_ySi_zO_4 + (0.5x + 1.5y)H_2O + (y + z - x)OH^- \xrightarrow{90^\circ C} xNa^+ + zSiO_3^= + yAl(OH)_4^- + zH^+ \qquad \text{(Eq. 6)}$$

Equation 6 creates free H^+. The amount of the H^+ released by these reactions will depend on the amount of each of these phases present and the values of the atomic ratios of Na:Al:Si, e.g. *x*, *y*, and *z*. In particular, Equation 5 when applied to the sample with beta alumina and unreacted SiO_2 is very dependent on the relative amounts of each of these phases present. The H^+ released serves to further buffer the solution pH in addition to the pH consumed by the aqueous complex $Al(OH)_4^-$. Thus the more alumina present in a sample, the more aluminosilicate buffering effects the leachate pH. For nepheline (*x*=*y*=*z*=1) one mole of H^+ is created. For some of the defect NAS phases between 0.55 to 1.1 moles of free H^+ can be generated to further buffer the leachate pH.

The leaching of the STAR 2003 SBW samples are highly governed by aluminosilicate buffering since more Al rich mineral phases were found in the 2003 FBSR products relative to the other products (Table II and Table III). The STAR 2003 SBW samples have a PCT pH of ~10.6 (Fig. 1a). The leaching of the STAR 2004 LAW bed samples (1103 and 1104) are also governed by aluminosilicate buffering as they contain both stoichiometric carnegieite and an Si-rich nepheline (Table III). Note that the STAR 2004 LAW fines leachate pH is ~12 (FBSR product 1125). This pH is higher (Fig. 1a) than the bed LAW 1103 and 1104 bed products because they are less well buffered. This is confirmed by the fact that the fines contain only a "trace" of the Si-rich nepheline instead of major quantities as in the bed samples (Table III). For comparison, the leaching of the Hazen 2002 AN-107 sample is governed by the aluminosilicate buffering of stoichiometric and Na-rich nepheline (Table III). The Hazen 2002 fines (PR-01) are governed by the stoichiometric nepheline and carnegieite aluminosilicate reactions (Equations 3, 5 and 6). This bed material had the highest pH of all the samples tested indicating that very little leachate buffering was occurring.

Fig. 1b-c shows that the Na and Cs are highly related to the Al release while Fig. 1d shows that Cs, Na, and Al release are parabolic functions of the leachate pH. The elements Re, S, and Si are linear functions of the leachate final pH (Fig. 1d) as controlled by the aluminosilicate buffering reactions discussed above. The Re-pH correlation has an R^2=0.83, the S-pH correlation has an R^2=0.96, and the Si-pH correlation (not shown) has an R^2=0.94. Because the Re, S, and Si release are each strongly correlated to pH, the releases are highly correlated to each other. The release sequence for all bed and fines samples tested between 2001 and present are S>Re>Na~Cs>Al>Si (Fig. 1d).

Table IV. Density and Measured BET Surface Area (SA_{BET}) of FBSR Products and Glass

Sample	Density by Pycnometry (g/m^3)	SA_{BET} (m^2/g)
July 2003 SBW CAMPAIGNS		
Bed 260, Bed 272, Bed 277	3.30×10^{-6}, 3.13×10^{-6}, 2.73×10^{-6}	6.03
August 2004 LAW CAMPAIGNS		
Bed 1103 and Bed 1104[a]	2.53×10^{-6}	4.53
Bed 1123	2.53×10^{-6}	4.43
Fines 1125	2.46×10^{-6}	4.41
October 2004 SBW CAMPAIGNS		
Bed 1173	2.76×10^{-6}	2.36
Hazen LAW CAMPAIGNS		
Bed SCT-02	2.66×10^{-6}, 2.764×10^{-6} [1]	2.37 [1]
PR-01 Fines	2.50×10^{-6}	5.15
Low Activity Reference Material (LRM)		
LRM Glass	Not Measured	0.04

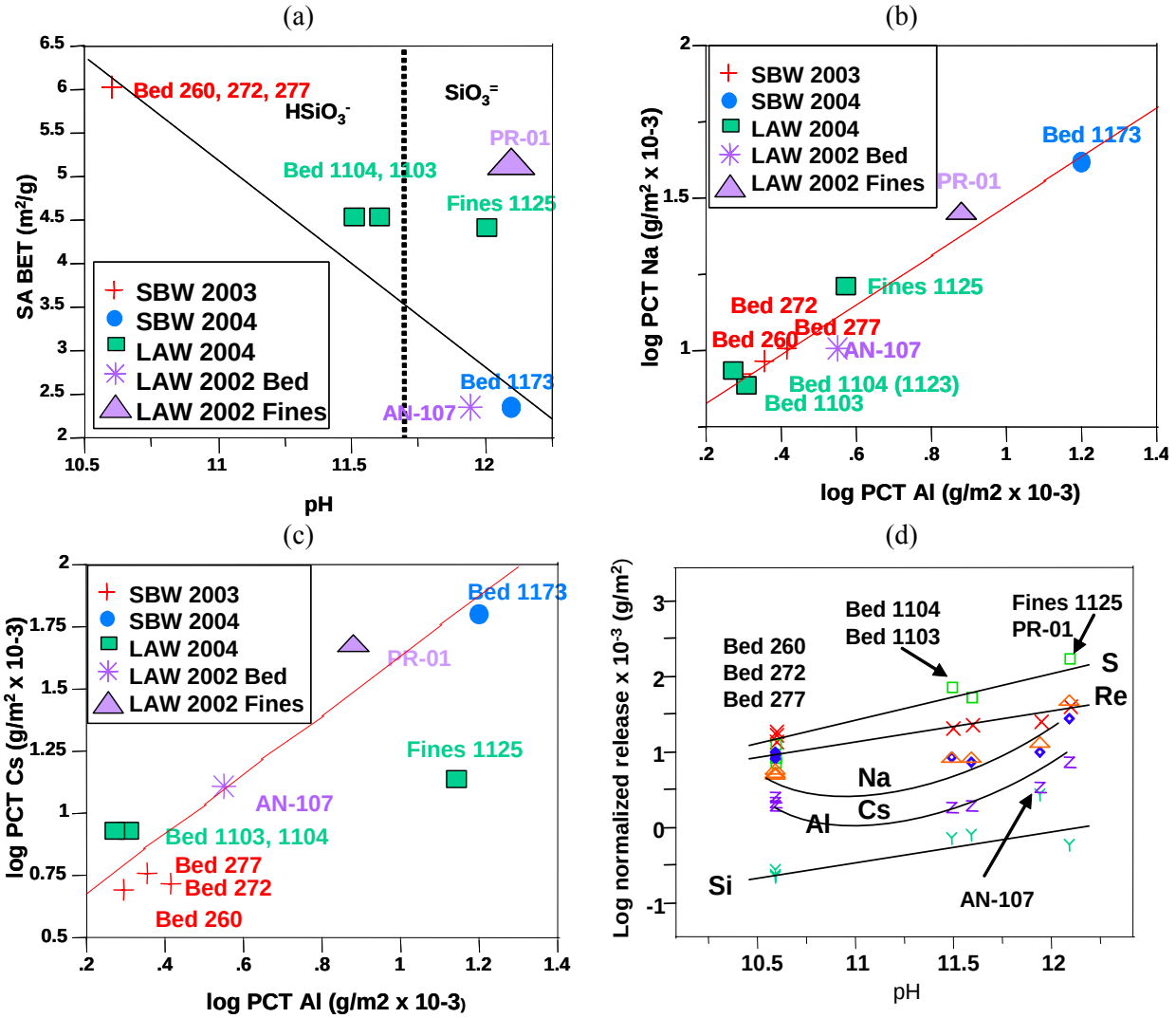

Fig. 1. Dependence of (a) pH on exposed surface area, (b, c) normalized alkali (Na and Cs) and Al released to solution, and (d) pH dependence of all the species on pH

Note that the NL_i release values given in Fig. 1 as log of element "i" are multiplied by 10^{-3} g/m^2. This indicates that the PCT release in normalized mass fraction, NL_i (normalized by the surface area given in Equation 1) is >2 orders of magnitude less than the Hanford specification of NL_{Na} =NL_{Re}=NL_{Tc}= 2 g/m^2 Na for Hanford LAW glass. If the PCT releases are expressed as NC_i (without the usage of the SA/V term in Equation 1 then the release of the SPFT product is equivalent to that of LAW glass.

Single Pass Flow Through Testing and Aluminosilicate Effects

The SPFT data of Lorier, et.al. [30] for Hanford and INL FBSR bed products was measured at 5 different pH values and 4 different temperatures for 3-14 day test durations. The plots of NR_i vs test duration given by Lorier, et. al. [30] demonstrate that steady state conditions were achieved between 8-14 day test durations at the high flow rates used. The 8-14 day NR_i values for each element from replicate tests were averaged in this study and plotted against pH in Fig. 2: each data point represents six replicate measurements used to determine steady state release rates of Si, Al, Na, Re (simulant for Tc-99) and S in a manner analogous to that of Knauss et. al. [34] for borosilicate waste glasses.

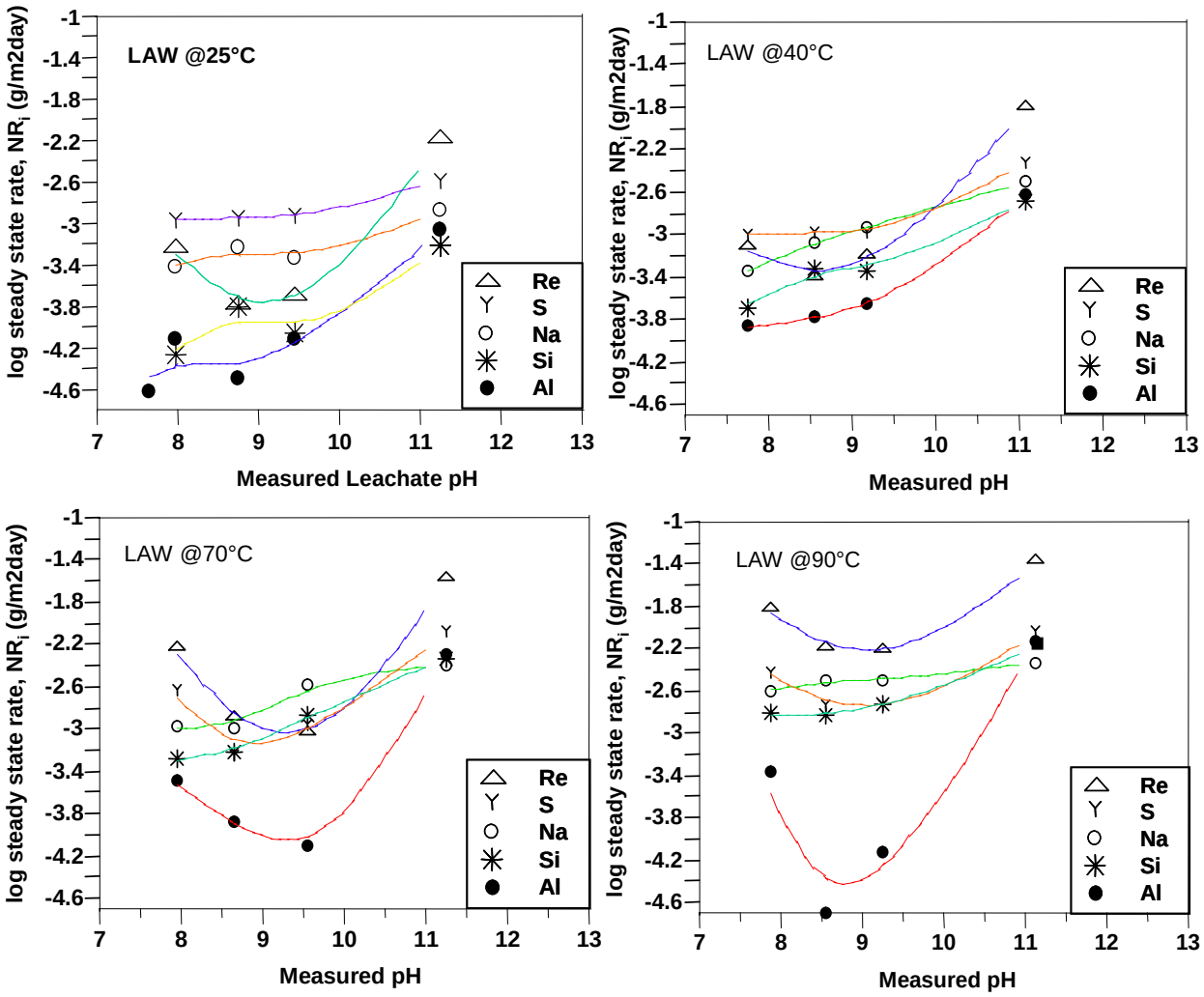

Fig. 2. Dependence of steady state (8-14 day) normalized alkali (Na), Al, Re, S and Si on solution pH

Fig. 2 shows that during SPFT testing of the LAW bed product that Re, Al and S dissolution is parabolic with solution pH, while Na and Si release are almost linear. In general at temperatures >25°C, the release sequence is Re>S~Na>Si>Al. This data suggests that the aluminum, rhenium, and sulfur dissolution are related, perhaps from dissolution of the nosean/sodalite phase while the dissolution of silicon and sodium appear independent of which felspathoid $Na[AlSiO_4]$ configuration is dissolving. This indicates that the dissolution may only be partially incongruent[3] [35] since the FBSR mineral phases are all aluminosilicates of the feldspathoid family with similar $Na[AlSiO_4]$ structural ratios.

It should be noted that the steady state release rates calculated in this study at flow rates of 288 mL/day are consistently lower than those reported by McGrail et.al. [1] for the 2002 LAW FBSR product at flow rates of 200 mL/day. While McGrail et al. state that at flow rates ≥140 mL/day, that the release rates become independent of the flow rate and should represent a true forward rate of reaction, their data for nepheline dissolution at flow rates between 60 and 100 mL/day indicate that the dissolution of Al, Si, and Na are similar. At the higher flow rates used in this study, Al dissolution is always lower than that of Si and Na and the lowest Al dissolution occurs at pH values between 8.5 and 9.5 in the 70-90°C temperature range (Fig. 2). This pH is the pH of the aqueous equilibrium boundary between amorphous $Al(OH)_3$ gel (which may be colloidal) and the aqueous species $Al(OH)_4^-$ [16]. Although colloidal species are not anticipated at these high flow rates it should be noted that the leachates in this study were filtered in case of particle carryover from the leach vessel but the leachates in the McGrail et al. [1] study were not filtered.

Other test parameters that varied between the testing by McGrail et.al. [1] and the test parameters in this study were (1) McGrail et.al. [1] manually removed the charcoal which Pariezs et al [11] determined leaves ~4 wt% charcoal in the product which alters the measured BET surface area and (2) McGrail et.al. N_2 purged their leachant reservoirs which was not done in the current study. However, the dissolution data calculated in this study (Fig. 3) for the dissolution of nosean and nepheline following the methodology in McGrail et.al. [1] gave a nosean dissolution rate of -3.20 and pH dependence of the rate (η) reaction order of 0.17 pH based on Re release and a rate of -3.45 and η=0.13 pH based on S release (McGrail et al. used S release only). In addition, the nepheline dissolution rate calculated was -6.39 with η=0.25 for Na and an η=0.30 for Si in agreement with the value of η=0.25 determined by McGrail [1].

The parabolic dependence of the Re, Al and S releases are still apparent in the leachate response observed during SPFT testing of the INL SBW FBSR mineral products although the parabolic dependency is not as well defined as in the LAW leachate response. The SBW FBSR mineral assemblages have sodalite and a K-substituted nepheline instead of the nosean and Na-nepheline phases predominant in the LAW FBSR products (see Table III). This may indicate that the LAW FBSR mineral assemblages are more difficult to dissolve and thus require higher flow rates than tested by Lorier et. al. [30] or McGrail et.al. [1]. For the SBW FBSR products the release sequence is S>Na>Si>Al>Re indicating that the Re may be captured in a different mineral phase than in the LAW FBSR products, e.g. it may be in a lower oxidation state (+4 instead of +7) since the REDOX ratio of the 2004 SBW campaign FBSR products was 0.81 versus 0.28 for the 2004 LAW campaign products. Therefore, Re in the SBW campaigns may be present as ReO_2 while it is in the nosean phase as $NaReO_4$ in the LAW campaigns.

---

[3] Incongruent dissolution of a waste form means that some of the dissolving species are released preferentially compared to others. Incongruent dissolution is often diffusion-controlled and can be either surface reaction-limited under conditions of near saturation or mass transport-controlled. Preferential phase dissolution, ion-exchange reactions, grain-boundary dissolution, and dissolution-reaction product formation on surfaces are among the more likely mechanisms of incongruent dissolution, which will prevail, in a complex polyphase ceramic waste form [35]. Congruent dissolution of a waste form, like glass, is the dissolving of species in their stoichiometric amounts. For congruent dissolution, the rate of release of a radionuclide from the waste form is proportional to (1) the dissolution rate of the waste form and (2) the relative abundance of the radionuclide in the waste form. Thus for borosilicate glass ^{99}Tc is released at the same rate, congruently, as Na, Li and B.

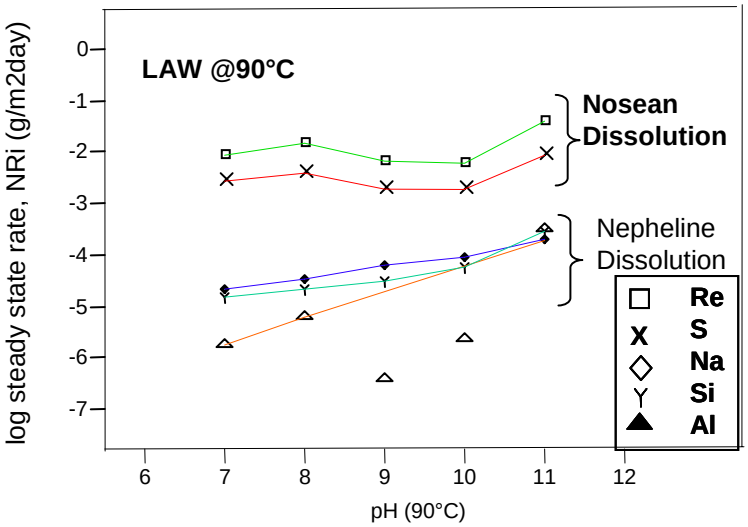

Fig. 3. Dissolution of nosean and nepheline in the Hanford LAW FBSR mineral waste form determined from SPFT testing

CONCLUSIONS

Fluidized Bed Steam Reformer (FBSR) products (bed and fines) were determined to be 2 orders of magnitude more durable than LAW glass when PCT and/or SPFT durability is expressed units of NL_i or NR_i, e.g. this is well below the NL_{Na}=2 g/m^2 release for LAW glass required by the Hanford glass durability specification. The PCT releases are comparable to LAW glass if expressed in units of NC_i. The two orders of magnitude durability finding is consistent with the findings of McGrail [1] during SPFT testing and Pressurized Unsaturated Flow (PUF) testing and Performance Assessment. [1, 36]

REFERENCES

1. McGrail, B.P.; Schaef, H.T.; Martin, P.F.; Bacon, D.H.; Rodriguez, E.A.; McCready, D.E.; Primak, A.N.; Orr, R.D. (2003). *Initial Evaluation of Steam-Reformed Low Activity Waste for Direct Land Disposal*; U.S. DOE Report PNWD-3288.
2. Jantzen, C.M. (2004). *Characterization and Performance of Fluidized Bed Steam Reforming (FBSR) Product as a Final Waste Form*; Ceramic Transactions 155, 319-329.
3. Jantzen, C.M. (2002). *Engineering Study of the Hanford Low Activity Waste (LAW) Steam Reforming Process*; U.S. DOE Report WSRC-TR-2002-00317.
4. Marshall, D.W.; Soelberg, N.R.; Shaber, K.M. (2003). *THOR^{sm} Bench-Scale Steam Reforming Demonstration*; U.S. DOE Report INEEL/EXT.03-00437.
5. Jantzen, C.M. (2003). *Disposition of Tank 48H Organics by Fluidized Bed Steam Reforming (FBSR)*; U.S. DOE Report WSRC-TR-2003-00352.
6. Jantzen, C.M. (2005). *Fluidized Bed Steam Reforming of Organic and Nitrate Containing Salt Supernate*, Ceramic Transactions 168, 68-79.
7. Soelberg, N.R.; Marshall, D.W.; Bates, S.O; Siemer, D.D. (2003). *SRS Tank 48 Steam Reforming Proof-of-Concept Test Results*; INEEL/EXT-03-01118.
8. J.B. Mason, J. McKibben, J. Ryan, J. Schmoker, (2003). *Steam Reforming Technology for Denitration and Immobilization of DOE Tank Wastes,* Waste Mgt. 03.

9. Soleberg, N.R.; Marshall, D.W.; Bates, S.O.; Taylor, D.D. (2004). *Phase 2 THOR Steam Reforming Tests for Sodium Bearing Waste Treatment*; U.S. DOE Report INEEL/EXT-04-01493.

10. ASTM C1285. Annual Book of ASTM Standards, Vol. 12.01: Standard Test Methods for Determining Chemical Durability of Nuclear, Hazardous, and Mixed Waste Glasses and Multiphase Glass Ceramics: The Product Consistency Test (PCT).

11 . Pareizs, J.M., Jantzen, C.M., Lorier, T.H. (2005). *Durability Testing of Fluidized Bed Steam Reformer (FBSR) Waste Forms for High Sodium Wastes at Hanford and Idaho*, U.S. DOE Report WSRC-TR-2005-00102.

12. Jantzen, C.M., Pareizs, J.M., Lorier, T.H. and Marra, J.M. (2005). Durability Testing of Fluidized Bed Steam Reforming (FBSR) Products, Ceramic Transactions, 176, 121-137 (2005).

13. Olson, A.L.; Soelberg, N.R.; Marshall, D.W.; Anderson, G.L. (2004). *Fluidized Bed Steam Reforming of Hanford LAW Using THOR^{sm} Mineralizing Technology*; U.S. DOE Report INEEL/EXT-04-02492.

14. Olson, A.L., Soleberg, N.R., Marshall, D.W. and Anderson, G.L. (2004) *Fluidized Bed Steam Refomring of INEEL SBW Using THOR^{sm} Mineralizing Technology,* U.S. DOE Report INEEL/EXT-04-02564.

15. Deer, W.A.; Howie, R.A.; Zussman, J. (1963). *Rock-Forming Minerals, Vol IV and Vol V*; John Wiley & Sons, Inc.: NY.

16. Brookins, D.G. (1984) *Geochemical Aspects of Radioactive Waste Disposal*; Springer-Verlag: NY, 347pp.

17. Ch Buhl, J.; Englehardt, G.; Felsche, J. (1989). Synthesis, X-ray Diffraction, and MAS n.m.r. Characteristics of Tetrahydroxoborate Sodalite, *Zeolites*, 9, 40-44.

18. Fleet, M.E. (1989). Structures of Sodium Alumino-Germanate Sodalites," *Acta Cryst.*, C45, 843-7.

19. Sinkler, W.; O'Holleran, T.P.; Frank, S.M;. Richmann, M.K.; Johnson, S.G. (2000). Characterization of a Glass-Bonded Ceramic Waste Form Loaded with U and Pu, *Sci.Basis Nucl. Waste Mgt., XXIII*, Mat. Res. Soc.: Pittsburgh, PA, 423-429.

20. Moschetti, T.L.; Sinkler, W.; DiSanto,T.; Novy, M.H.; Warren, A.R.; Cummings, D.; Johnson, S.G.; Goff, K.M.; Bateman, K.J.; Frank, S.M., (2000). Characterization of a Ceramic Waste Form Encapsulating Radioactive Electrorefiner Salt, *Sci.Basis Nucl. Waste Mgt., XXIII*, Mat. Res. Soc., Pittsburgh, PA, 577-582.

21. Berry, L.G. and Mason, B. (1959). *Mineralogy Concepts, Descriptions, Determinations*; W.H. Freeman & Co.: San Francisco, CA, 630pp.

22. Klingenberg, R. and Felsche, J. (1986). Interstitial Cristobalite-type Compounds $(Na_2O)_{0.33}Na[AlSiO_4])$, *J. Solid State Chemistry*, 61, 40-46.

23. Huang, D; Drummond, III, C.H.; Wang, J.; Blume, R.D.(2004). Incorporation of Chromium (III) and Chromium (VI) Oxides in a Simulated Basaltic, Industrial Waste Glass-Ceramic, *J. Am. Ceram. Soc*. 87 [11], 2047-2052.

24. Land Disposal Restricions (2004). Code of Federal Regulations, Part 268, Title 40.

25. Bullock, Jr., J.H; Cathcart, J.D.; Betterton, W.J. (2002). *Analytical methods utilized by the United States Geological Survey for the Analysis of Coal and Coal Combustion By-products*; US Geological Survey: Denver, CO.

26. Crow, R.F.; Connolly, J.D. (1973). Atomic Absorption Analysis of Portland Cement and Raw Mix Using Lithium Metaborate Fusion, *Jour. Test. Evaluation*, 1, 382.

27. ASTM C1463. Annual Book of ASTM Standards, Vol. 12.01: Practice for Dissolving Glass Containing Radiactive and Mixed Waste for Chemical and Radiochemical Analysis

28. ASTM C1317. Annual Book of ASTM Standards, Vol. 12.01: Standard Practice for Dissolution of Silicate or Acid-Resistant Matrix Samples.

29. Baumann, E.W. (1992). Colorimetric Determination of Iron (II) and Iron (III) in Glass," *Analyst*, 117, 913-6.

30. Lorier, T.H., Pareizs, J.M. and Jantzen, C.M. (2005). *Single Pass Flow Through (SPFT) Testing of Fluidized Bed Steam Reforming (FBSR) Waste Forms*, U.S. DOE Report, WSRC-TR-2005-00124.

31. Brunauer, S.; Emmett, P.H.; Teller, E., (1938). Adsorption of Gases in Multimolecular Layers. *Journal of Physical Chemistry,* 60:309-319.

32. ASTM D1193. Annual Book of ASTM Standards, Vol. 11.01: Specification for Reagent Water.

33. Schreiber, H.D., Schreiber, C.W., Donald, S.B., Mayhew, K.M., Stokes, M.E., and Swink, A.M. (2005). Redox State of Model Fluidized Bed Steam Reforming Systems, Am. Cer. Soc. Abs. #AM-S21-22, p. 199.

34. Knauss, K.G., Bourcier, W.L., McKeegan, K.D., Merzbacher, C.I., Nguyen S.N., Ryerson, F.J., Smith, D.K, Weed, H.C. and Newton, L. (1990). Dissolution Kinetics of a Simple Analogue Nuclear Waste Glass as a Function of pH, Time and Temperature, *Sci.Basis Nucl. Waste Mgt., XIII*, MRS., Pittsburgh, PA, 371-381.

35. Jantzen, C.M., Clarke, D.R., Morgan, P.E.D. and Harker, A.B. "Leaching of Polyphase Nuclear Waste Ceramics: Microstructural and Phase Characterization," J. Am. Ceram. Soc. 65[6], 292-300 (1982).

36. McGrail, B.P. (2003). *Laboratory Testing of Bulk Vitrified and Steam-Reformed Low-Activity Forms to Support a Preliminary Assessment for an Integrated Disposal Facility*; U.S. DOE Report PNNL-14414.